Probing the Composition of Ge Dots and Si1-xGex Island Superlattices

Baribeau, Jean-Marc; Wu, X.; Lockwood, David

Publisher's version / Version de l'éditeur:
https://doi.org/10.1116/1.2186658
Journal of Vacuum Science and Technology A, 24, 3, pp. 663-667, 2006

Probing the composition of Ge dots and $Si/Si_{1-x}Ge_x$ island superlattices

J.-M. Baribeau,[a] X. Wu, and D. J. Lockwood
Institute for Microstructural Sciences, National Research Council Canada, Ottawa, Ontario K1A 0R6, Canada

(Received 19 August 2005; accepted 13 February 2006; published 4 May 2006)

We use analytical transmission electron microscopy to map the composition of Ge dot and $Si/Si_{1-x}Ge_x$ island structures grown on (001) Si by molecular beam epitaxy or ultrahigh vacuum chemical vapor deposition. Energy-dispersive x-ray spectroscopy reveals that nominally pure Ge dots grown by molecular beam epitaxy at 650 °C exhibit considerable intermixing with the average Ge composition typically increasing from nearly zero at the base to about 50% at the top of the dot. In pyramid shaped dots, the Ge composition increases linearly up to the top of the dot, while for dome dots, a saturation of the incorporation rate is seen beyond a distance of 7 nm from the substrate interface. Probing of $Si/Si_{1-x}Ge_x$ island superlattices also reveals large Si/Ge intermixing with a Ge accumulation at the crest and Ge depletion at the troughs of the islands. These results are corroborated by x-ray diffraction and Raman scattering measurements. © *2006 American Vacuum Society.* [DOI: 10.1116/1.2186658]

I. INTRODUCTION

The study of semiconductor three-dimensional (3D) islands and quantum dots has been a very active area of research in the last decade. In particular, Ge dots and $Si/Si_{1-x}Ge_x$ island superlattices on (001) Si have emerged as prototypical model systems for the study of self-assembly of semiconductor nanostructures.[1–3] Although the nucleation, size distribution, and evolution of Ge dots and $Si_{1-x}Ge_x$ islands are now fairly well understood, there remain questions concerning the chemical and strain profiles within these nanostructures. A better knowledge of these properties is crucial for the exploitation of these nanostructures in quantum devices.

Techniques such as x-ray scattering,[3] x-ray absorption,[4] atomic force microscopy,[5] transmission electron microscopy (TEM),[6] Raman scattering,[7] electron energy-loss spectroscopy (EELS),[8] and photoluminescence[9] have been used to probe the composition of individual or ensembles of Ge islands and dots. Although most results point to intermixing and an increase in Ge concentration towards the top of the dots, the actual Ge distribution within a single dot has not been fully mapped out without ambiguity. The chemical modulation within stacked $Si/Si_{1-x}Ge_x$ island superlattices has also not been investigated in any detail. Here, the analytical transmission electron microscopy is used to map the composition of various Ge dot and $Si/Si_{1-x}Ge_x$ island structures grown by molecular beam epitaxy (MBE) or ultrahigh vacuum chemical vapor deposition (UHV-CVD). The measurements confirm that considerable intermixing takes place within nominally pure Ge dots. Furthermore it is found that pyramid- and domelike dots exhibit different concentration profiles both in the growth direction and parallel to the interface. The probing of $Si/Si_{1-x}Ge_x$ island superlattices reveals intermixing in the growth direction as well as lateral diffusion of Ge in the structures. These results are corroborated by x-ray diffraction and Raman scattering spectroscopy measurements.

II. EXPERIMENTAL DETAILS

The $Si/Si_{1-x}Ge_x$ heterostructures were prepared on (001) Si by MBE (VG Semicon V80)[10] or by UHV-CVD (Leybold Syrius).[11] The Ge dots were grown by MBE by depositing ~6 ML of Ge at a temperature of 650 °C and a growth rate of 0.05 nm s^{-1}. The MBE grown $Si/Si_{1-x}Ge_x$ island superlattice structure was grown at 625 °C and consisted of ten periods of Si (13.7 nm) and $Si_{1-x}Ge_x$ (4 nm, $x=0.48$) layers. The UHV-CVD grown $Si/Si_{1-x}Ge_x$ island superlattice was comprised of ten periods of alternating $Si_{1-x}Ge_x$ (4 nm) and Si (12.5 nm) layers with a nominal Ge composition of $x=0.6$. This structure was grown at 525 °C, with deposition rates of 0.02 nm s^{-1} for the Si spacer layers, and of 0.067 nm s^{-1} for the $Si_{0.4}Ge_{0.6}$ layers. The MBE and UHV-CVD temperatures were calibrated by infrared pyrometry to a ±25 °C accuracy.

The TEM work was performed on a JEOL JEM-2100F field emission source transmission electron microscope operating at 200 kV. For the present study high-angle annular dark field (HAADF) scanning TEM images were obtained using a Fischione annular dark field detector attached to the JEM-2100F. The chemical composition of the various Si/Ge nanostructures was studied quantitatively by scanning transmission electron microscope energy-dispersive x-ray spectroscopy (STEM-EDS) using an Oxford INCA Energy TEM 200 using a probe size of 0.7 nm. Spectra were recorded with sample drift compensation and calibrated by probing thick $Si/Si_{1-x}Ge_x$ heterostructures of known germanium composition. The thickness of the TEM cross-section samples was measured by electron energy loss spectroscopy (Gatan GIF Tridiem) using standard methodology.[12] The sample regions investigated were typically 50–60 nm thick.

[a]Author to whom correspondence should be addressed; electronic mail: jean-marc.baribeau@nrc.ca

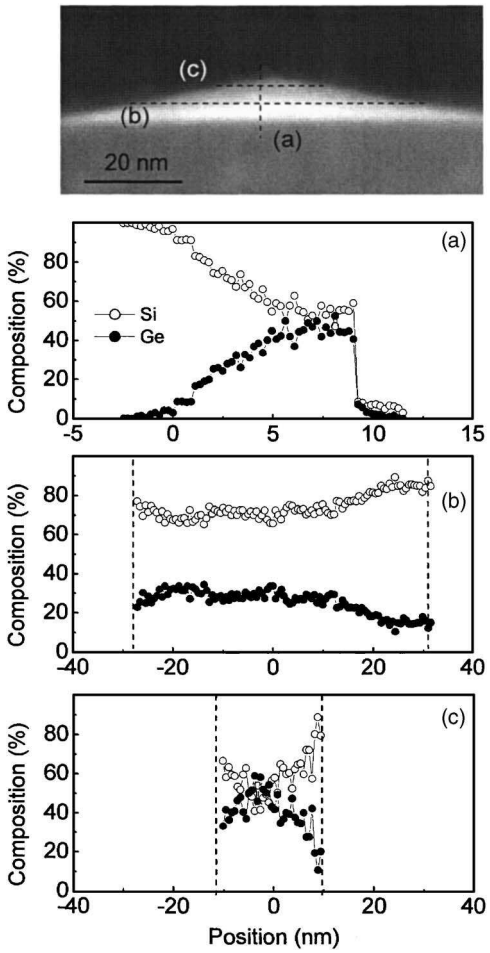

FIG. 1. STEM HAADF image of a pyramid Ge dot on (001) Si and EDS chemical profile line scans measured along the dotted lines indicated. The dotted lines in panels (b) and (c) indicate the dot boundary.

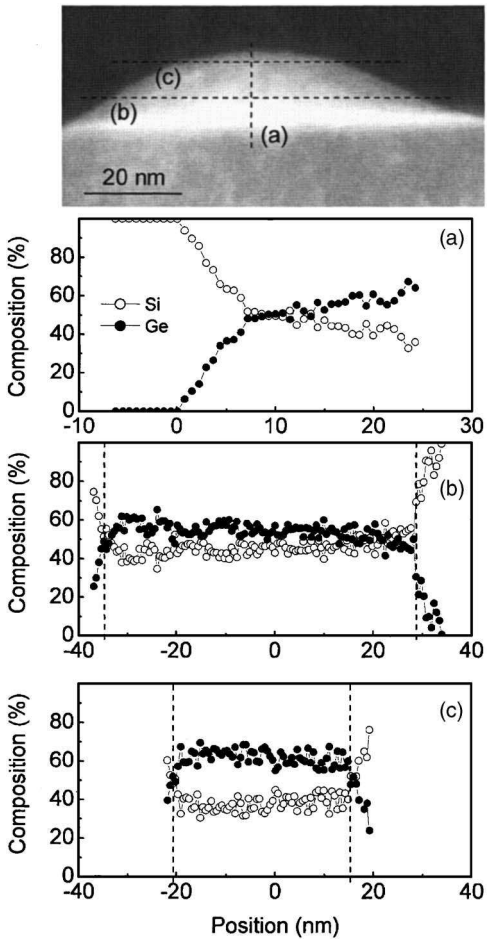

FIG. 2. STEM HAADF image of a dome Ge dot on (001) Si and EDS chemical profile line scans measured along the dotted lines indicated. The dotted lines in panels (b) and (c) indicate the dot boundary.

The Raman scattering experiments were carried out in an ambient atmosphere of helium at a temperature of 295 K in a quasibackscattering Brewster angle geometry.[13] The 457.9 nm incident light was polarized in the scattering plane, while the scattered light was recorded without polarization analysis. X-ray diffraction (400) rocking curves from island superlattices were recorded on a Philips MRD system equipped with a four-bounce Ge (220) monochromator.

III. RESULTS AND DISCUSSION

A. Ge pyramid and dome dots

Analytical TEM techniques have recently been used to investigate the structure and composition of Ge nanostructures.[14] Figure 1 displays a HAADF micrograph of a pyramid dot along with the Ge concentration profiles measured by STEM-EDS line scans along the growth direction and parallel to the wafer surface. Considerable Si–Ge intermixing is observed with the dot Ge concentration increasing almost linearly from close to 0 at the base to about 0.5 at the apex of the pyramid. The EDS scans in the direction parallel to the interface suggest that at a given height, there is a small Ge depletion at the periphery of the dot.

Similar measurements for a dome dot are shown in Fig. 2. Here the Ge concentration increases in the growth direction at a rate similar to that of pyramid dots to reach about $x=0.4$ at a 5 nm height. Beyond that point, however, the Ge concentration only builds up slowly over the remaining $\sim$20 nm to reach $x=0.6$ at the top of the dome. In the case of dome dots, the Ge concentration at a given height was found to be remarkably uniform laterally, as is shown in Fig. 2 for two particular line scans parallel to the surface.

Before discussing those results, it is important to note that all the TEM samples examined were submitted to a final ion-milling treatment to form a thin wedge (6° angle) oriented parallel to the sample surface. All the EDS scans perpendicular to the layered structures are thus done at a constant thickness (typically about 50 nm). For scans parallel to the surface, the thickness variation is small (less than 5 nm or 10%) across the width sampled and this may have introduced a small sloping background in the lateral scans of quantum dots (Figs. 1 and 2). This, however, does not invalidate the general conclusions of the analysis. Note that the use of thinner TEM sections could lead to erroneous results if the peak of the quantum dot has been milled away.

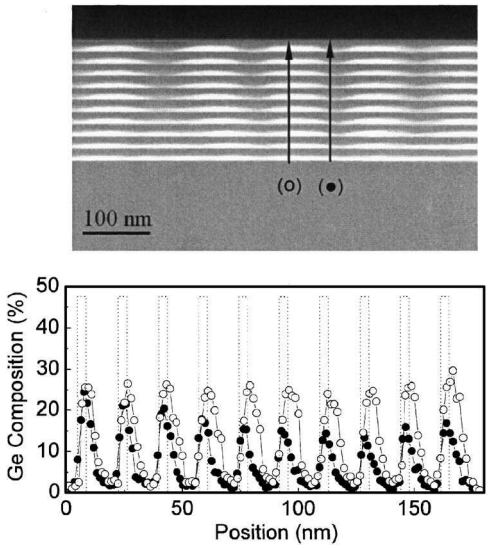

FIG. 3. STEM HAADF image of a $Si/Si_{1-x}Ge_x$ island superlattice grown by MBE on (001) Si and EDS chemical profiles in the growth direction measured along an interface crest (open circles) and along an interface valley (full circles). The nominal average Ge concentration profile as determined by x-ray diffraction is shown by the dotted line.

The results obtained here corroborate the earlier studies that point to considerable intermixing in dots grown at high temperatures. In particular, the vertical concentration profile and lateral uniformity in the dome island is in excellent agreement with an EELS study of the Ge island concentration of dome islands as a function of temperature.[15] The results are also in agreement with the anomalous x-ray scattering measurements[16] that showed a rapid increase of the Ge concentration in the dots in the first 2 nm from the surface. The line profiles parallel to the surface are useful to determine whether the dots can be modelled by a shell model with the Ge composition decreasing radially towards the centre of the dot or by a lamellar structure where the Ge gradient is perpendicular to the dot/substrate interface. For both types of dots, our data points to a lamellar structure rather than a shell-like structure predicted in atomistic simulations[17] or inferred from x-ray scattering studies.[18] A comparison of the composition profiles in Figs. 1 and 2 shows differences exist in the Ge profile in the growth direction between dome and pyramid dots prepared under identical growth conditions. The stronger intermixing in the pyramid is likely mediated by strain as these dots remain heavily tetragonally distorted in comparison to the domes that adopt a relaxed lattice constant close to that of bulk Ge near the top of the dot.

B. $Si/Si_{1-x}Ge_x$ island superlattices

The concentration profile in the growth direction in island superlattices was also investigated by STEM-EDS. Figure 3 compares the Ge profiles in the growth direction measured along a crest and a trough in the MBE grown island superlattice. As was observed in the dot structures, large Si–Ge intermixing takes place in the island superlattice. The maximum Ge concentration is about 0.25 along the crests and only 0.15–0.20 along the troughs. This peak concentration is less than the nominal value of $x=0.48$ due to a broadening of the Ge profile that spreads within the Si spacer layers. The integrated Ge signal per superlattice period at a crest is, however, close to that of the nominal structure. In the troughs, the Ge concentration is significantly reduced and the integrated Ge signal corresponds to approximately 50% of that of a nominal superlattice period, indicating significant surface lateral diffusion during growth. The Ge profiles in Fig. 3 also point to the Ge surface segregation, as evidenced by an exponential decay of the Ge concentration at the trailing edge of the $Si_{1-x}Ge_x$ layers. The decay length, is about 3.3 nm, in good agreement with the values reported for planar $Si/Si_{1-x}Ge_x$ heterostructures.[19] The decay of the total Ge content in successive troughs also indicates higher chemical contrast and better defined Ge-rich islands as growth progresses, as is also seen in the HAADF image of Fig. 3. There is, however, no evidence of a decay of the Ge peak concentration in the crest in the upper layers as has been reported in similar structures.[20]

By contrast, in the UHV-CVD grown sample, the Ge profile in the each superlattice period exhibits a symmetrical triangular shape indicating that interdiffusion takes place at both the leading and trailing interfaces of the $Si_{1-x}Ge_x$ alloy layers. The decay length of the Ge concentration is about 2.5 nm and there seems to be no appreciable Ge segregation, possibly because of the surfactant effect of hydrogen created by the dissociation of silane and germane during growth. For the line scan performed along a superlattice crest, the integrated Ge signal is equivalent to a Ge composition of 0.48, which is less than that of the nominal composition of $x=0.6$, based on growth parameters. In comparison, the line scan along a trough shows a depletion of the Ge signal that corresponds to an equivalent Ge concentration of 0.35. Variations in the Ge composition from period to period are also seen in the UHV-CVD sample. The undulation of both types of interfaces progressively leads to a loss of registry of the superlattice period with respect to the nominal structural parameters, a phenomenon that is not observed with MBE. The average Ge composition is significantly lower than the nominal value expected from growth calibrations in steady-state conditions. This can only be explained by transients in the Si/Ge incorporation rates when the Ge flow is switched on and off affecting the nominal composition of very thin films. The lack of self-organization of the undulations as compared to the MBE case may be due to the surfactant effect of surface hydrogen and lower growth temperature both inhibiting lateral mass transport.

In the case of the wavy superlattices, again the TEM samples are thin enough (50 nm) so that in the scans of the wave crest perpendicular to the surface, only the SiGe wave is probed and not the surrounding Si. The fact that there is no significant variation in the height of the SiGe crests for adjacent self-assembled waves in Figs. 3 and 4 also suggests that the island center is included in the foil or the dot section in the foil is at least very close to it. It is possible that in the case of perpendicular scans along a valley, a small amount of

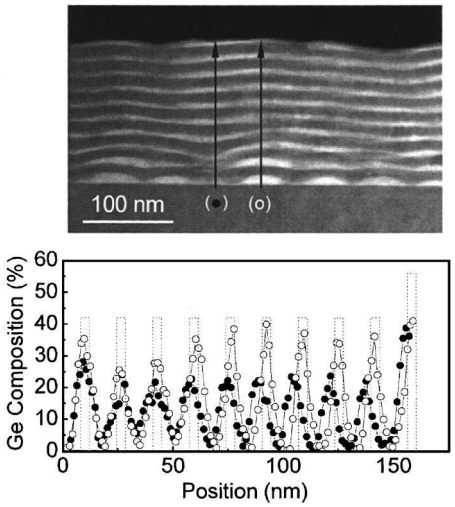

FIG. 4. STEM HAADF image of a $Si/Si_{1-x}Ge_x$ island superlattice grown by UHV-CVD on (001) Si and EDS chemical profiles in the growth direction measured along an interface crest (open circles) and along an interface valley (full circles). The nominal average Ge concentration profile as determined by x-ray diffraction is shown by the dotted line.

surrounding Si is also probed. This may have contributed to the apparent Ge depletion measured in the valleys.

C. X-ray diffraction and Raman scattering

The island superlattices discussed above were also investigated by x-ray diffraction. Figure 5 presents (400) rocking curves from the MBE and UHV-CVD grown superlattices. In both cases, the simulation profiles are also displayed. Curves (*b*) are the best fits to experiment, assuming planar interfaces, calculated using the composition profile shown by the dotted line in Figs. 3 and 4 for the MBE and UHV-CVD cases, respectively. For the MBE sample, the rocking curve is consistent with the presence of 3.7-nm-thick $Si_{1-x}Ge_x$ layers with $x=0.475$, in excellent agreement with the nominal growth parameters. In the UHV-CVD sample, the best fit is

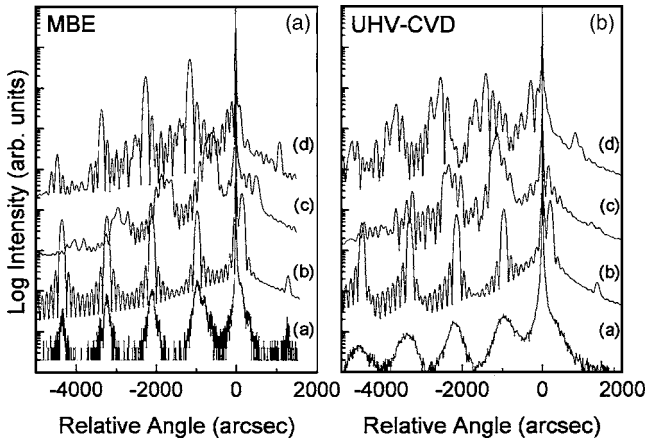

FIG. 5. (a) Measured (004) x-ray rocking curves from the MBE (left) and UHV-CVD (right) $Si/Si_{1-x}Ge_x$ island superlattices and simulated curves calculated for a planar structure (b) and for the Ge concentration profile in the trough (c) and crest (d) as determined by STEM-EDS.

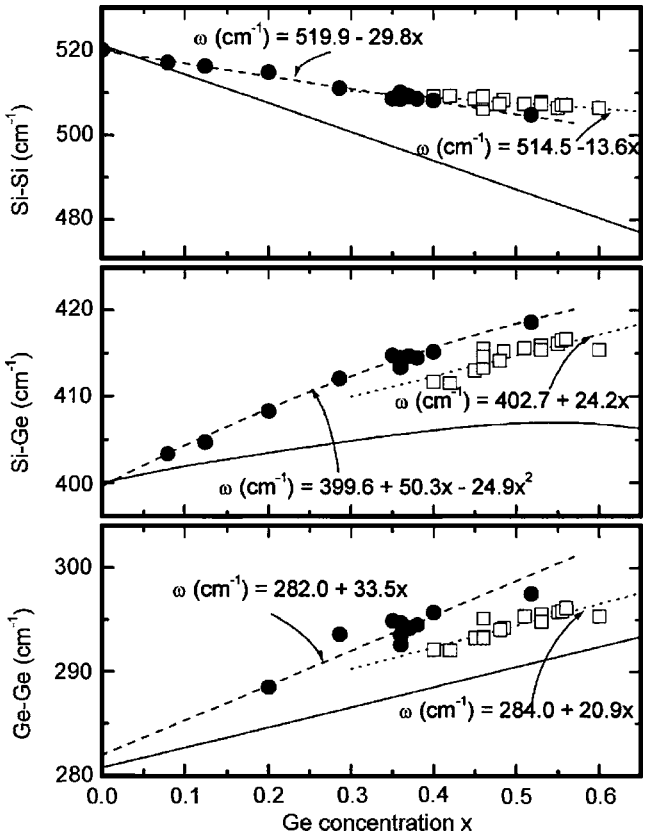

FIG. 6. Frequencies of the three optic modes in $Si/Si_{1-x}Ge_x$ island superlattices (open circles) and planar superlattices (solid circles) as a function of composition x. The solid lines are for bulk material (Ref. 21).

obtained with $Si_{1-x}Ge_x$ layers 4 nm thick and with $x=0.42$, confirming a significantly lower Ge content than the nominal value as concluded from the STEM-EDS study. For both samples, the experimental satellite peaks show considerable broadening arising from the undulation of the interfaces and lateral variations in the Ge composition. Simulations (*c*) and (*d*) were calculated using the composition profiles determined by STEM-EDS at the wave peak and trough, respectively, and show to what extent the satellites are expected to shift and their line shape to be altered by composition and thickness modulations. A superposition of intensity profiles reflecting the lateral nonuniformity of the superlattice is consistent with the peak broadening observed.

Raman spectroscopy has been widely applied to characterizing the strain and composition of $Si_{1-x}Ge_x$ dots grown epitaxially on Si.[2] In the Raman spectrum of $Si_{1-x}Ge_x$, vibrational modes appear at approximately 500, 400, and 300 cm^{-1}, associated with the Si–Si, Si–Ge, and Ge–Ge lattice vibrations. The Si–Si (Ge–Ge) mode frequency decreases (increases) linearly with x, while the Si–Ge mode behavior is best represented by a fourth order polynomial.[21] All three optical modes are sensitive to the presence of strain, which causes a shift in their mode frequencies.[22]

In Fig. 6, the frequencies of the three optic modes are displayed as a function of x-ray determined x for the strained planar superlattice on Si (solid circles),[21] island superlattice

grown by MBE (open circles) and unstrained alloy (solid lines). The long (short) dashed lines in Fig. 6 are from fits of the planar (island) superlattice mode frequencies to linear or quadratic functions of x. It shows that the three mode frequencies in the island superlattice behave as a function of x quite differently from those in both the unstrained bulk alloy and strained planar superlattices. This indicates that apart from strain and composition other factors such as island size, distribution, and shape[23] might have to be taken into account in analyzing the behaviors of the optic phonon mode frequencies in an island or dot nanostructure. The results presented here are consistent with an accumulation of Ge at the crest of the undulations that produces a decrease of the Ge fraction in the continuous alloy layers between the islands thereby causing an overall shift down in frequency for the alloy vibration modes. In fact, the Si–Ge and Ge–Ge vibrational frequencies in the undulated case are close to those measured in planar superlattices with about a 10% lower nominal Ge concentration, consistent with analytical TEM results. The out diffusion of Ge results in Si rich alloy regions in the valleys (between the $Si_{1-x}Ge_x$ crests) that are under compression. This contributes to shifting the Si–Si line frequency above the expected nominal value for a given "average" concentration x.

IV. CONCLUSION

In summary, STEM-EDS has proven to be an effective technique to probe the atomic distribution within Ge dots and $Si_{1-x}Ge_x$ island superlattices. For Ge dots obtained by deposition of pure Ge on (001) Si, the measurements show that atomic diffusion during growth results in considerable intermixing. Larger intermixing is found at the base of the dots, but the concentration at the top of the Ge dots grown at 625 °C was found to not exceed 55%–60%. Also, the composition of dome dots was found remarkably uniform laterally, while a small Ge depletion near the edges of the dots was measured in pyramid dots. STEM-EDS also confirmed the lateral composition variations in $Si_{1-x}Ge_x$ island superlattices characterized by the accumulation of Ge at the crest of the interface undulations. Interesting differences in the atomic distribution of analogous structures grown by MBE and UHV-CVD were revealed.

[1]B. Teichert, Phys. Rep. **365**, 335 (2002).
[2]J.-M. Baribeau, N. L. Rowell, and D. J. Lockwood, in *Self-Organized Nanoscale Materials*, edited by M. Adachi and D. J. Lockwood (Springer, New York, 2006), p. 1.
[3]A. Stangl, V. Holý, and G. Bauer, Rev. Mod. Phys. **76**, 725 (2004).
[4]F. Boscherini, G. Capellini, L. Di Gaspare, F. Rosei, N. Motta, and S. Mobilio, Appl. Phys. Lett. **76**, 682 (2000).
[5]C. J. Huang, D. Z. Li, Z. Yu, B. W. Cheng, J. Z. Yu, and Q. M. Wang, Appl. Phys. Lett. **77**, 391 (2000).
[6]C. P. Liu, J. M. Gibson, D. G. Cahill, T. I. Kamins, D. P. Basile, and R. S. Williams, Phys. Rev. Lett. **84**, 1958 (2000); X. Z. Liao, J. Zou, D. J. H. Cockayne, Z. M. Jiang, and X. Wang, J. Appl. Phys. **90**, 2725 (2001).
[7]M. Cazayous *et al.*, J. Appl. Phys. **91**, 6772 (2002); V. Magidson, D. V. Regelman, R. Beserman, and K. Dettmer, Appl. Phys. Lett. **73**, 1044 (1998).
[8]M. Floyd, Y. Zhang, K. P. Driver, J. Drucker, P. A. Crozier, and D. J. Smith, Appl. Phys. Lett. **82**, 1473 (2003).
[9]U. Denker, H. Sigg, and O. G. Schmidt, Mater. Sci. Eng., B **101**, 89 (2003).
[10]J. M. Baribeau, T. E. Jackman, D. C. Houghton, P. Maigné, and M. W. Denhoff, J. Appl. Phys. **63**, 5738 (1988); J.-M. Baribeau, J. Cryst. Growth **157**, 52 (1995).
[11]H. Lafontaine, D. C. Houghton, D. Elliott, N. L. Rowell, J.-M. Baribeau, S. Laframboise, G. I. Sproule, and S. J. Rolfe, J. Vac. Sci. Technol. B **14**, 1675 (1996); H. Lafontaine, N. L. Rowell, S. Janz, and D.-X. Xu, J. Appl. Phys. **86**, 1287 (1999).
[12]D. B. Williams and C. B. Carter, *Transmission Electron Microscopy IV Spectrometry* (Plenum, New York, 1996).
[13]D. J. Lockwood, M. W. C. Dharma-wardana, J.-M. Baribeau, and D. C. Houghton, Phys. Rev. B **35**, 3243 (1987).
[14]C.-P. Liu, R. D. Twesten, and J. Murray Gibson, Ultramicroscopy **87**, 79 (2000); D. Miller, C.-P. Liu, and J. Murray Gibson, *ibid.* **84**, 225 (2000); T. J. V. Yates, L. Laffont, D. Zhi, and P. A. Midgley, in *Electron Microscopy and Analysis Group Conference, EMAG2003*, edited by S. McVitie and D. McComb (Institute of Physics, Oxford, 2004), Vol. 179, pp. 31; D. Zhi, P. A. Midgley, R. E. Dunin-Borkowski, B. Joyce, D. W. Pashley, A. L. Bleloch, and P. J. Goodhew, in *Group-IV Semiconductor Nanostructures*, edited by L. Tsybeskov *et al.* (Materials Research Society, Pittsburgh, 2005), Vol. 832, pp. F5.4.1; D. Zhi *et al.*, in *Electron Microscopy and Analysis Group Conference, EMAG2003*, edited by S. McVitie and D. McComb (IOP, Oxford, 2004), Vol. 179, pp. 39.
[15]D. J. Smith, D. Chandrasekhar, S. A. Chaparro, P. A. Crozier, J. Drucker, M. Floyd, M. R. McCartney, and Y. Zhang, J. Cryst. Growth **259**, 232 (2003).
[16]T. U. Schülli, J. Stangl, Z. Zhong, R. T. Lechner, M. Sztucki, T. H. Metzger, and G. Bauer, Phys. Rev. Lett. **90**, 066105 (2003); R. Magalhaes-Paniago, G. Medeiros-Ribeiro, A. Malachias, S. Kycia, T. I. Kamins, and R. Stanley Williams, Phys. Rev. B **66**, 245312 (2002).
[17]C. Lang, D. J. H. Cockayne, and D. Nguyen-Manh, Phys. Rev. B **72**, 155328 (2005).
[18]A. Malachias, S. Kycia, G. Medeiros-Ribeiro, R. Magalhaes-Paniago, T. I. Kamins, and R. Stanley Williams, Phys. Rev. Lett. **91**, 176101 (2003).
[19]S. Fukatsu, K. Fujita, H. Yaguchi, Y. Shiraki, and R. Ito, Appl. Phys. Lett. **59**, 2103 (1991); G. Ohta, S. Fukatsu, Y. Ebuchi, T. Hattori, N. Usami, and Y. Shiraki, *ibid.* **65**, 2975 (1994).
[20]O. G. Schmidt, U. Denker, S. Christiansen, and F. Ernst, Appl. Phys. Lett. **81**, 2614 (2002).
[21]H. K. Shin, D. J. Lockwood, and J.-M. Baribeau, Solid State Commun. **114**, 505 (2000).
[22]D. J. Lockwood and J.-M. Baribeau, Phys. Rev. B **45**, 8565 (1992); J.-M. Baribeau and D. J. Lockwood, in *Thin Films, Stresses and Mechanical Properties III*, edited by W. D. Nix *et al.* (Materials Research Society, Boston, 1992), Vol. 239, pp. 449.
[23]A. B. Talochkin and S. A. Teys, JETP Lett. **75**, 264 (2002); A. G. Milekhin, A. I. Nikiforov, M. Yu. Ladanov, O. P. Pchelyakov, S. Schulze, and D. R. T. Zahn, Phys. Solid State **46**, 92 (2004).